Bio-inspired controller achieving forward speed modulation with a 3D bipedal walker

Van der Noot et al. - 2018

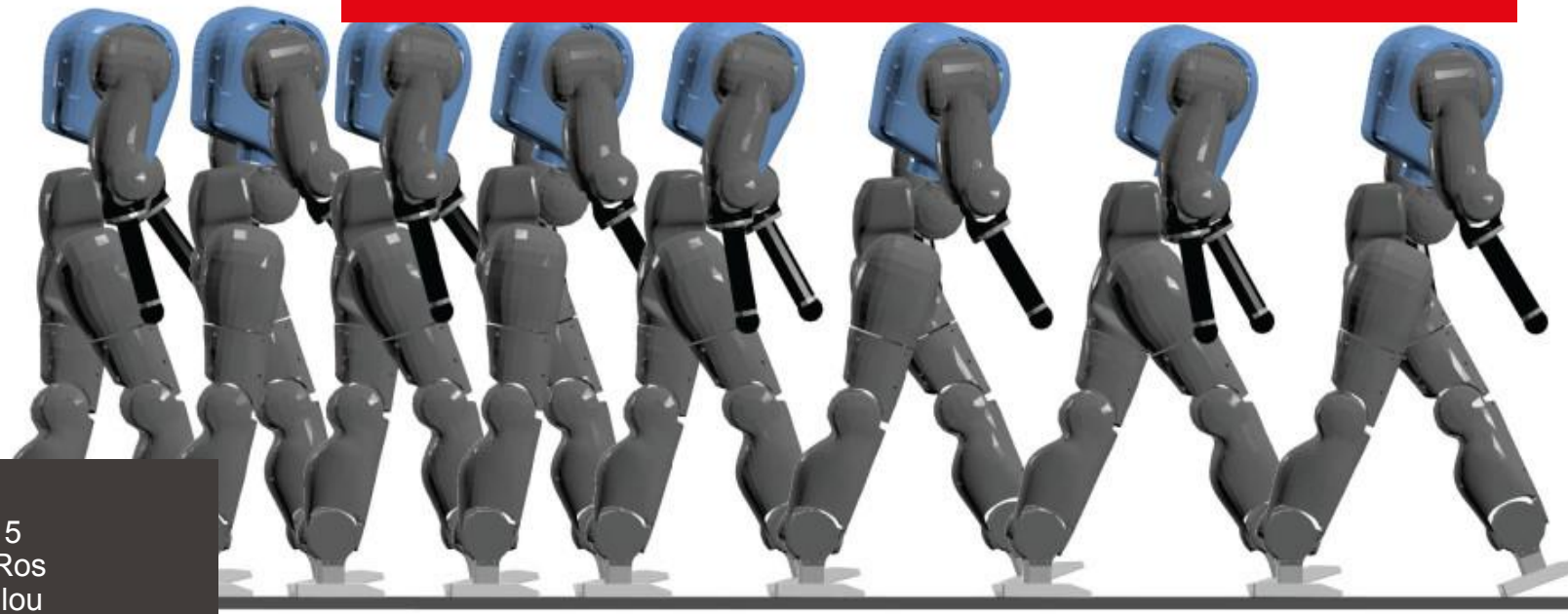

Group 15
Elias Da Ros
Selim Kellou
Julien Mangiatordi

MICRO-507 Legged Robots
Autumn 2025

After impact, the walker recovers its previous gait, thanks to the CPG entrainment.

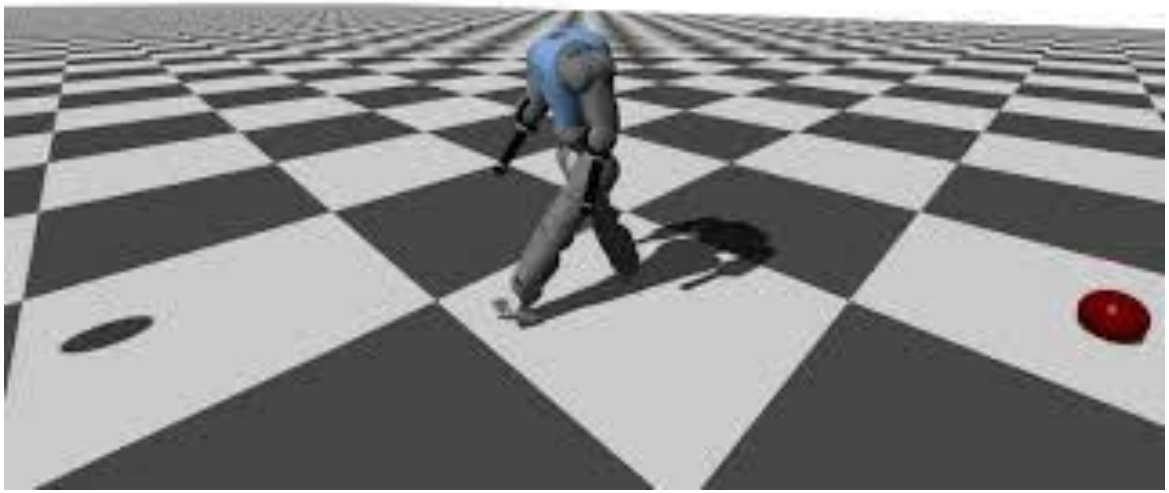

Robustness against external perturbation:
https://www.youtube.com/watch?v=volLoG7IhbE&list=PLpRT1DySTGyw9S_SMs23_V3-LEwdnWUXi&index=5

Group 15 : Elias Da Ros | Selim Kellou |Julien Mangiatordi

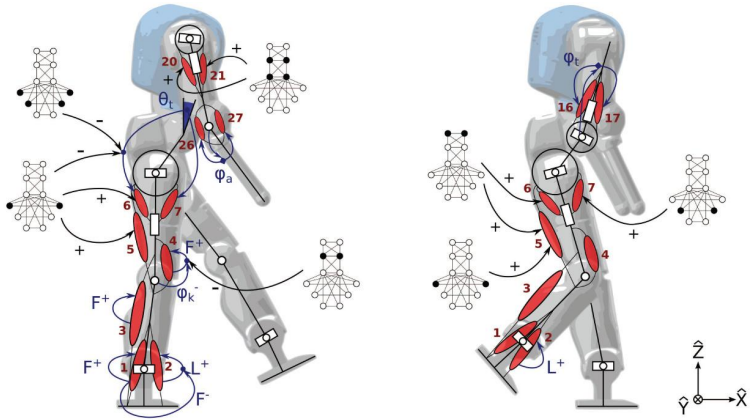

(a) Sagittal muscles (arm and stance leg)

(b) Sagittal muscles (torso and swing leg)

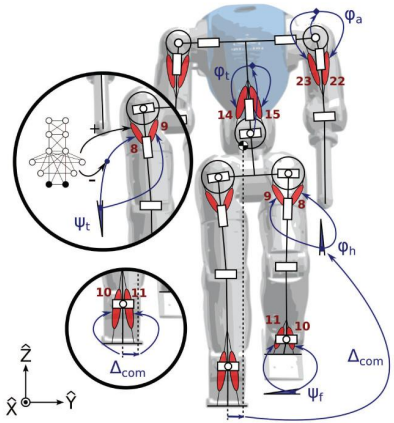

(d) Lateral muscles (arm, torso, and leg)

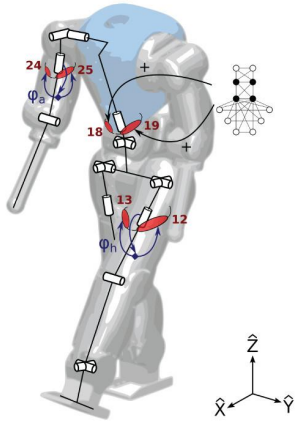

(e) Transverse muscles (arm, torso, and leg)

Outline

- Main Ideas
- Key Aspects
- Central Pattern Generator
- Optimization
- Results
- Conclusion

Main Ideas

- Bio-inspiration to achieve robust, energy-efficient and natural gaits

- Mix of Central Pattern Generator and reflexes-based controller

  Inspirational papers:
  - Reflexes-based controller: Geyer and Herr - 2010 [1]
  - CPG: Matsuoka - 1985/1987 [2] [3], Taga - 1994 [4]

- Forward speed modulation

Key Aspects

- Biped robot: COMAN model
- Torque control - Virtual Hill-type muscles forces
- Tuned using optimization - Particle Swarm Optimization
- Walking gait, with different speed
- Use of IMU, encoders and torque/force sensors

Group 15 : Elias Da Ros | Selim Kellou |Julien Mangiatordi

Key Aspects

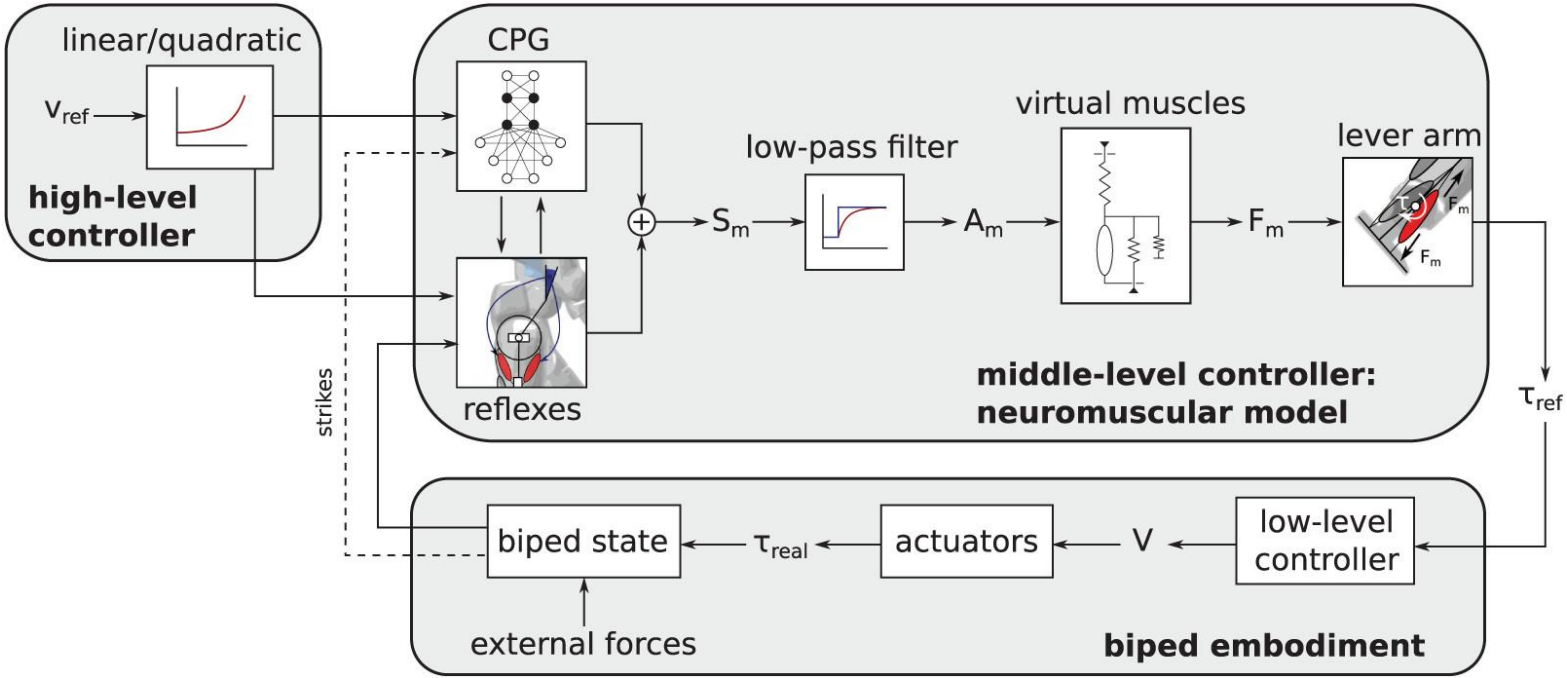

CPG: 12 neurons Matsuoka oscillator [2] [3]

Reflexes: closed-loop PD controller

Virtual muscles: Hill-type muscles (Hill - 1938) [5]

23 Joints - 27 Muscles

Group 15 : Elias Da Ros | Selim Kellou |Julien Mangiatordi

CPG

- **Rhythm Generator neurons** (RG): Neurons N1 - N4 - provide the main frequency and phasing of the gait cycle

- **Pattern Formation neurons** (PF): Neurons NA - NH - rely on RG to generate signals to shape muscles stimulation, each neuron corresponds to the activation of specific muscle(s)

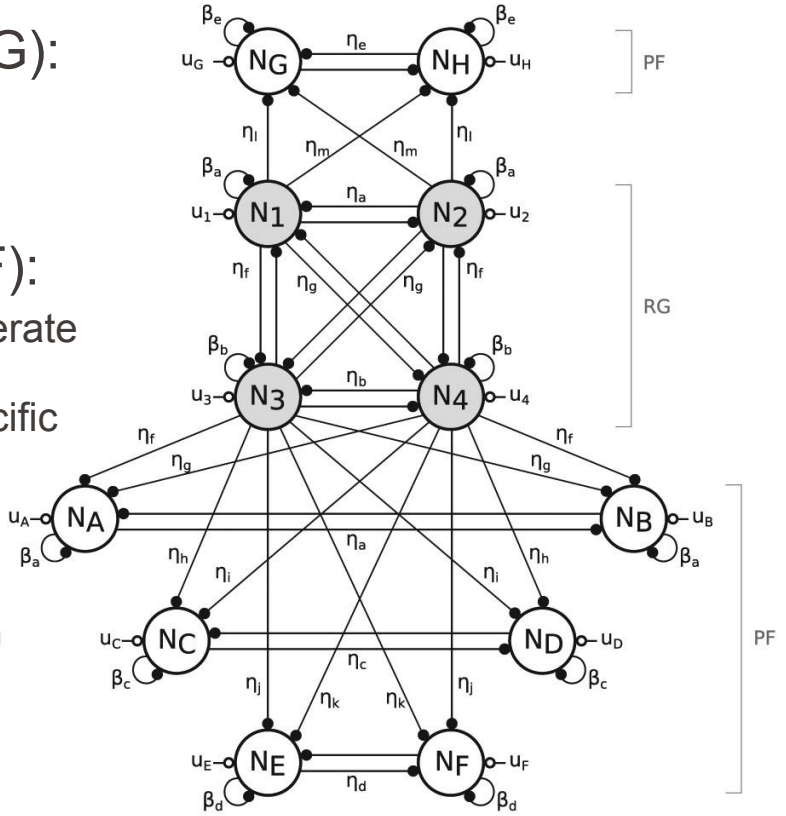

State equation:

$$\dot{x}_i = \frac{1}{\tau}\left(-x_i - \beta_j\, v_i - \sum \eta_k\, [x_l]^+ + u_i\right)$$

Self-inhibition:

$$\dot{v}_i = \frac{1}{\gamma_j\, \tau}\left(-v_i + [x_i]^+\right)$$

Group 15 : Elias Da Ros | Selim Kellou |Julien Mangiatordi

CPG

N1-N4:
- rhythm generation and upper-body control

NA-NB:
- knee bending and torso sagittal stabilization

NC-ND:
- hip flexion

NE-NF:
- torso lateral stabilizatior

NG-NH:
- late swing leg retraction

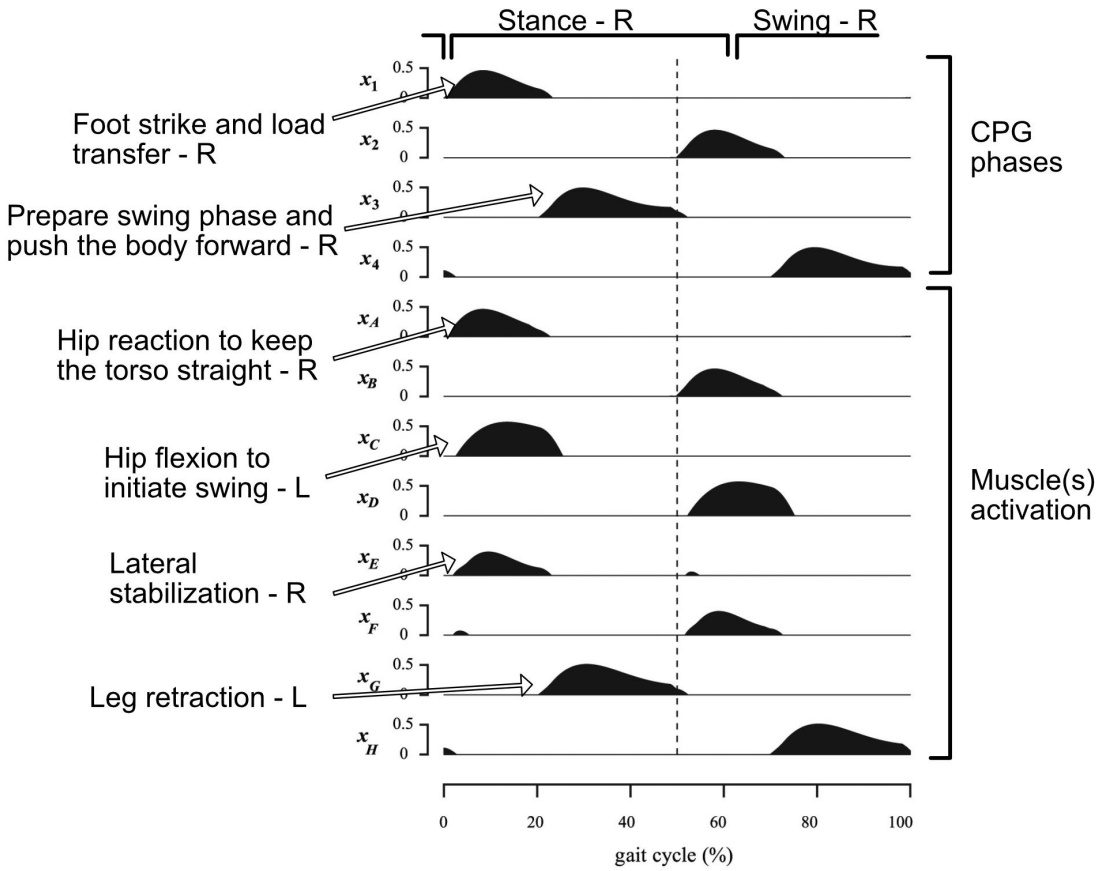

Group 15 : Elias Da Ros | Selim Kellou |Julien Mangiatordi

Optimization

- Method of optimization :
  - Algorithm: PSO
  - Max episode: 60 seconds or robot falling
  - Fitness function: $f = 100\, e^{-\alpha(x - x^*)^2}$

Walking	Walking for 60 seconds	Reaching target speed	Metabolic Efficiency, Gait Timing Accuracy, and Lateral Foot Placement Stability
The objective of this stage is to make the robot move forward. We use a reward proportional to distance traveled.	The objective of this stage is to make the robot walk for the entire episode. We use a reward proportional to the walked time.	We use the fitness function with $\alpha = 100$ and x^* the respective target speed. x is the speed of the robot,	We do three parallel optimizations. • Metabolic efficiency: x is the metabolic energy consumption. $\alpha = 10^{-3}$ and $x^* = 0$. • Gait Timing Accuracy: x is the mean error between the CPG predicted strike times and the actual ones . $\alpha = 250$ and $x^* = 0$. • Lateral Foot Placement Stability: x is average lateral distance between strike footprints. $f(x) = \begin{cases} 0, & x < 9\text{ cm} \\ 100, & x \geq 14\text{ cm} \\ 100\,\frac{x-9}{14-9} \end{cases}$

Group 15 : Elias Da Ros | Selim Kellou |Julien Mangiatordi

Optimization

- Experiment 1:

  Optimize all these parameters for the range 0.4 to 0.9 m/s speed with 0.05 m/s step. We have 11 controllers for the 11 different speeds.

Table 1. The parameters to be optimized in the controller and their ranges. The speed-dependent parameters are computed as follows: $\tau = K_\tau + L_\tau\, v_* + M_\tau\, v_*^2$; $k_{HAB} = K_{HAB} + L_{HAB}\, v_* + M_{HAB}\, v_*^2$; $k_{HFL} = K_{HFL} + L_{HFL}\, v_*$; $k_{GLU,1} = K_{GLU,1} + L_{GLU,1}\, v_*$; $k_{HAM,1} = K_{HAM,1} + L_{HAM,1}\, v_*$; $k_{HAM,2} = K_{HAM,2} + L_{HAM,2}\, v_* + M_{HAM,2}\, v_*^2$; $k_{HAM,3} = K_{HAM,3} + L_{HAM,3}\, v_*$; $\theta_{ref} = K_\theta + L_\theta\, v_*$; $\Lambda_{ref,h} = K_{\Lambda,h} + L_{\Lambda,h}\, v_* + M_{\Lambda,h}\, v_*^2$, where $v_* = v_{ref} - 0.65$ and v_{ref} is the target forward speed. When only a single speed was optimized, all the terms related to v_* and v_*^2 were removed. On top of that, the remaining speed parameters (i.e. labeled as $K_\bullet$) received a higher range, close to the bounds of the vertical axes of Figure 7. The parameters optimized for the reference controller are provided in Extension 1.

	min	max		min	max		min	max		min	max		min	max
β			η_e	4	6.5	$K_{HAM,1}$	2	3	$M_{\Lambda,h}$	0	0.3	$k_{d,\Lambda,h}$	0.1	0.4
β_a	5	6.5	η_f	2	4	$K_{HAM,2}$	0.4	1	**reflex (s)**			$k_{p,\varphi,h}$	3.5	5.5
β_b	3	4.5	η_g	3	4.5	$K_{HAM,3}$	0	0.1	G_{SOL}	0.85	1.05	$k_{d,\varphi,h}$	0.2	0.5
β_c	2.5	5	η_h	3.5	5	K_θ	0.18	0.25	$G_{SOL,TA}$	0.3	1	$k_{p,\Psi,f}$	12	18
β_d	4	6.5	η_i	3.5	5	$K_{\Lambda,h}$	0.04	0.09	$G_{TA,sw}$	1.5	4	$k_{d,\Psi,f}$	0.5	1
β_e	3	4.5	η_j	3.5	4.5	L_τ	-0.04	-0.01	$G_{TA,st}$	1.5	2.5	$k_{p,\Lambda,f}$	70	120
γ			η_k	3.5	5	L_{HAB}	-1	0.4	G_{GAS}	0.2	0.8	$k_{d,\Lambda,f}$	10	20
γ_a	2	4	η_l	2.5	3.5	L_{HFL}	2.5	4	G_{VAS}	25	35	$\Lambda_{ref,f}$	0.03	0.06
γ_b	2	3.5	η_m	3	4	$L_{GLU,1}$	0.2	1.5	$l_{TA,sw}$	0.8	0.9	**init**		
γ_c	2.5	5.5	**const**			$L_{HAM,1}$	3	7	$l_{TA,st}$	0.55	0.65	$T_{st,in}$	0.1	0.4
γ_d	1	2	$k_{GLU,2}$	0	0.15	$L_{HAM,2}$	-1.3	-0.3	$\varphi_{k,th}$	0	0.3	$T_{sw,in}$	0	0.3
γ_e	2.5	4	Ψ, ref	0.03	0.05	$L_{HAM,3}$	-0.35	-0.2	$k_{p,\theta}$	4	10	$S_{st,in}$	0.6	1
η			**speed**			L_θ	0.2	0.35	$k_{d,\theta}$	0.2	0.8	$S_{sw,in}$	0	0.5
η_a	3.5	6	K_τ	0.078	0.085	$L_{\Lambda,h}$	-0.04	0.06	**reflex (l)**			X_{init}	0.03	0.07
η_b	4.5	7	K_{HAB}	1.4	2.2	M_τ	-0.08	0	$k_{p,\Psi}$	10	15	Y_{init}	0	0.03
η_c	3.5	5.5	K_{HFL}	3.5	6	M_{HAB}	-1.5	0	$k_{d,\Psi}$	1.5	2.5	**upper**		
η_d	5.5	7	$K_{GLU,1}$	2.5	3.5	$M_{HAM,2}$	1	3	$k_{p,\Lambda,h}$	1	2.5	k_{torso}	0.07	0.11

Optimization

- Experiment 2:

  Apply the optimization for the same speed range with all parameters fixed except speed related ones and analyse the dependency. We select linear or quadratic function.

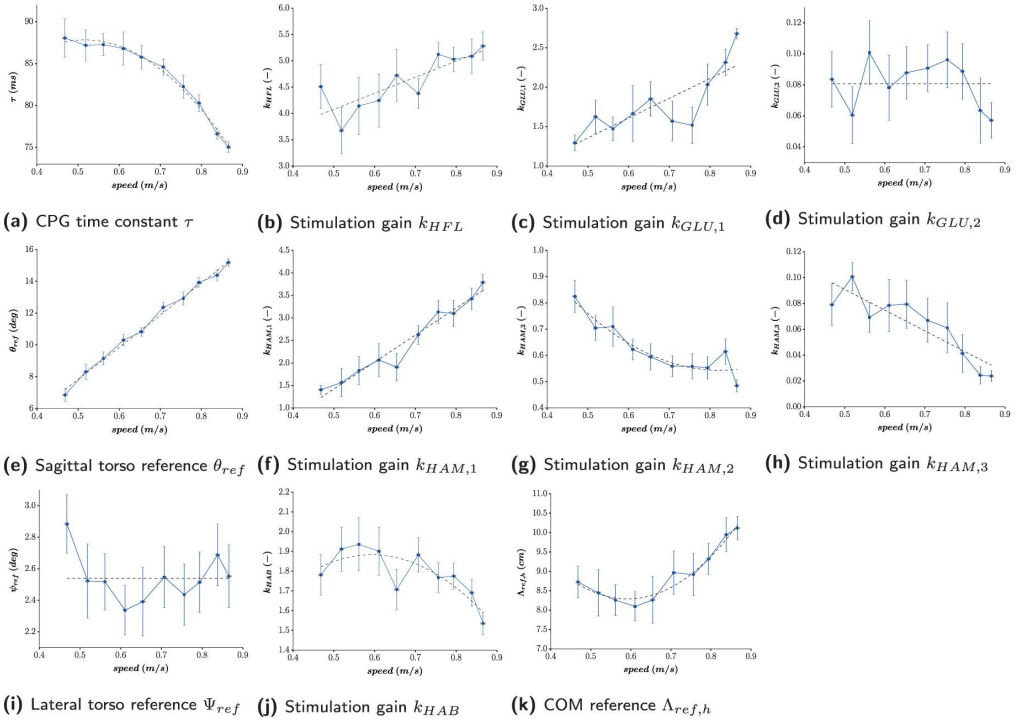

(a) CPG time constant τ (b) Stimulation gain k_{HFL} (c) Stimulation gain $k_{GLU,1}$ (d) Stimulation gain $k_{GLU,2}$

(e) Sagittal torso reference θ_{ref} (f) Stimulation gain $k_{HAM,1}$ (g) Stimulation gain $k_{HAM,2}$ (h) Stimulation gain $k_{HAM,3}$

(i) Lateral torso reference Ψ_{ref} (j) Stimulation gain k_{HAB} (k) COM reference $\Lambda_{ref,h}$

Group 15 : Elias Da Ros | Selim Kellou |Julien Mangiatordi

Optimization

- Experiment 3:

  We do a final optimization over all the speed range so we can have a single and stable controller. We optimize, this time, the linear or/and quadratic coefficients for the speed related parameters and all the others that we fixed in experiment 2 again.

- We have these formulas for the speed related parameters:

$$\tau = K_\tau + L_\tau v_* + M_\tau v_*^2;\ k_{HAB} = K_{HAB} + L_{HAB} v_* + M_{HAB} v_*^2;\ k_{HFL} = K_{HFL} + L_{HFL} v_*;\ k_{GLU,1} = K_{GLU,1} + L_{GLU,1} v_*;$$
$$k_{HAM,1} = K_{HAM,1} + L_{HAM,1} v_*;\ k_{HAM,2} = K_{HAM,2} + L_{HAM,2} v_* + M_{HAM,2} v_*^2;\ k_{HAM,3} = K_{HAM,3} + L_{HAM,3} v_*;\ \theta_{ref} = K_\theta + L_\theta v_*;$$
$$\Lambda_{ref,h} = K_{\Lambda,h} + L_{\Lambda,h} v_* + M_{\Lambda,h} v_*^2, \text{ where } v_* = v_{ref} - 0.65 \text{ and } v_{ref} \text{ is the target forward speed. When only a single speed was}$$

Group 15 : Elias Da Ros | Selim Kellou |Julien Mangiatordi

Results

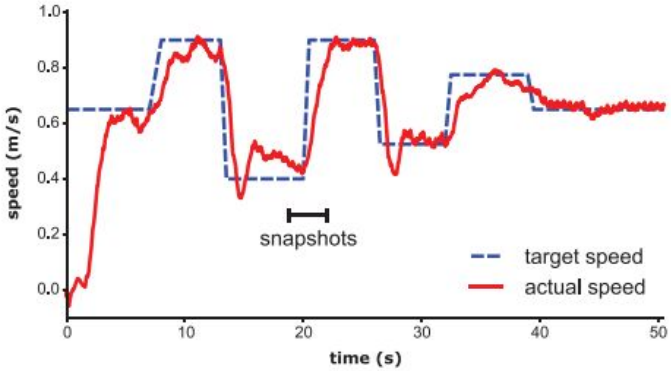

(b) Target speed tracking

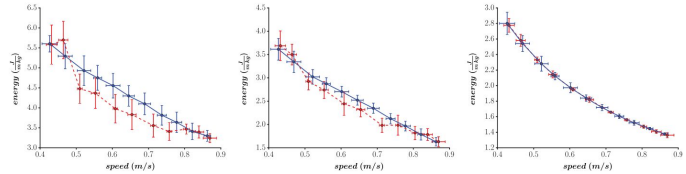

(a) Energy sagittal muscles (b) Energy lateral muscles (c) Energy transverse muscles

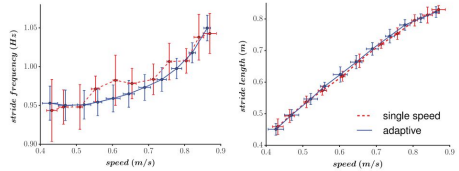

(d) Stride frequency (e) Stride length

- Fast adaptation: accelerations up to ±0.25 m/s² and less than two steps to go from minimum to maximum speed
- Energy per distance decreases as speed increases → faster gaits are more efficient.
- Stride length and frequency both increase with speed
- Adaptive controller is nearly as efficient as single-speed controllers, with consistent results across all speeds

Comparison with LIP controller and Human data

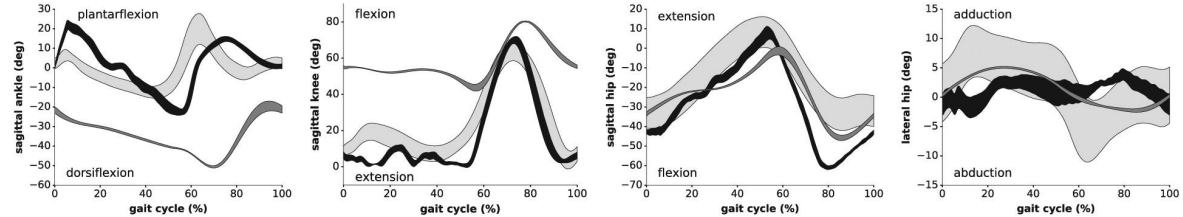

(a) Sagittal ankle angle (b) Sagittal knee angle (c) Sagittal hip angle (d) Lateral hip angle

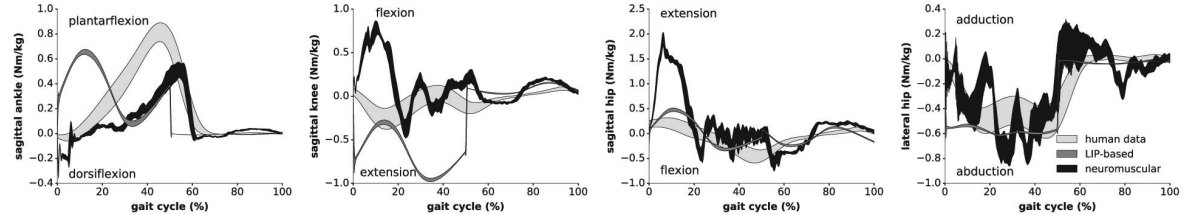

(e) Sagittal ankle torque (f) Sagittal knee torque (g) Sagittal hip torque (h) Lateral hip torque

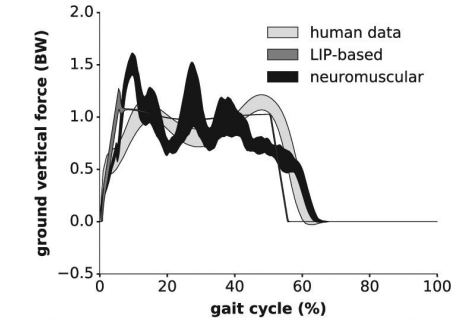

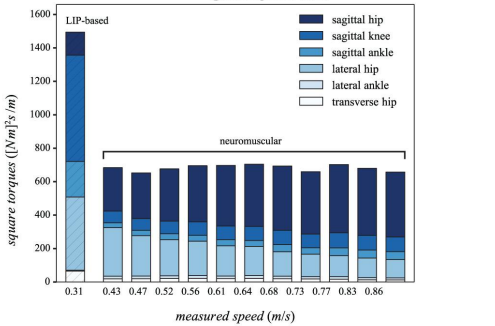

(b) Square torques per gait cycle, divided by traveled distance

- Knee and ankle angle profiles match human data; LIP controller shows significant deviations.
- Hip torques: neuromuscular R = 0.97 vs human; LIP produces larger peaks and phase shifts.
- Energy per distance : neuromuscular controller is ~2× more efficient than LIP across all speeds.
- At low speeds (< 0.64 m/s), neuromuscular joint torques are substantially lower than LIP, reducing energy demand.
- Ground reaction forces: neuromuscular produces human-like M-shaped vertical pattern; LIP shows quasi-flat profile.

Gaits Robustness

- Multi-environment robustness: no controller parameter changes required.
- CPG + reflexes: automatic synchronization after perturbations (phase entrainment).
- Stairs: automatic stride length adaptation, even when foot lands between steps.
- Slopes: up to 2.58° uphill, 2.29° downhill (scaled by speed).
- Irregular ground: walks over 25 mm tall obstacles without falling.
- External pushes: resists up to ~20 N at intermediate speeds.
- Blind walking: no environmental perception, full adaptation via sensory reflexes.

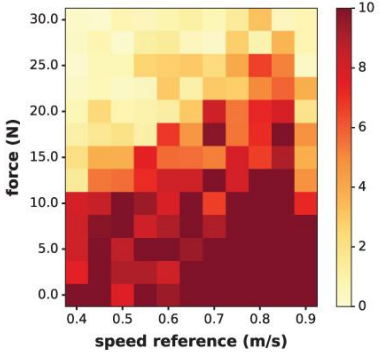

(a) Pushes on the torso

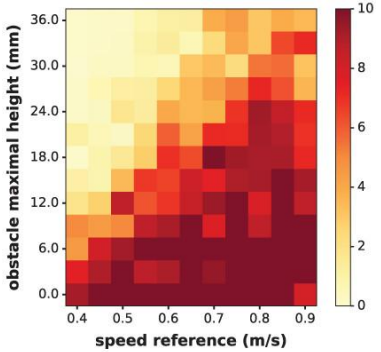

(b) Irregular ground

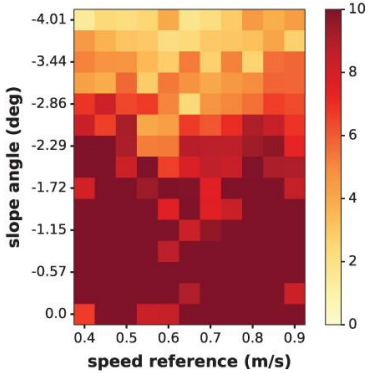

(a) Negative slopes

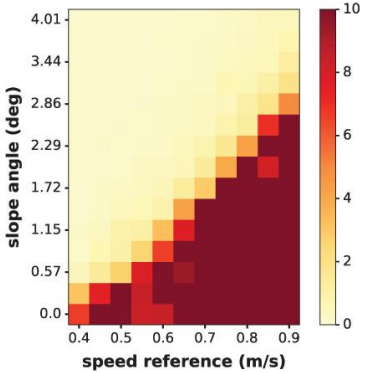

(b) Positive slopes

Group 15 : Elias Da Ros | Selim Kellou |Julien Mangiatordi

Results

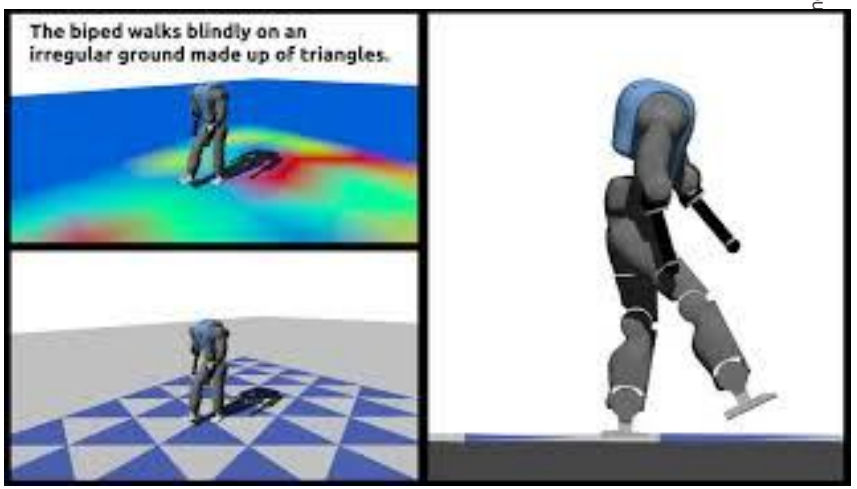

- Robustness against external perturbation:
  https://www.youtube.com/watch?v=volLoG7IhbE&list=PLpRT1DySTGyw9S_SMs23_V3-LEwdnWUXi&index=5
- Blind walking on irregular ground
  https://www.youtube.com/watch?v=xvsswU4ikqw&list=PLpRT1DySTGyw9S_SMs23_V3-LEwdnWUXi&index=2

Conclusion

Pros:

- More robust and energy efficient than model-based controllers
- Low computational cost, good for real-time applications
- Generated gaits are closer to human-like locomotion (proximo-distal hypothesis)
- No need to know the dynamic model of the robot

Cons (or possible improvement):

- Use of rigid feet with very different mechanical properties with regard to human feet
- Upper body muscles controlled directly by the RG neurons, extra PF neurons could offer better performances
- Adding fall detection to increase the robustness
- Implementing a high-level controller to modulate the CPG inputs to generate desired gaits
- Only walking gait

Group 15 : Elias Da Ros | Selim Kellou |Julien Mangiatordi

Conclusion

- Citation: 29 citations, mostly cited as example of CPG and reflex implementation or to mention the use of Hill muscles

  Examples of similar approaches:
  - Addition of preactivation reflex to increase robustness: Bunz et al. - 2023 [6]
  - The inverse CPG model is constructed based on neural network along with autoencoder: Park et al. - 2020 [11]
  - Adaptive oscillators used for locomotive assistance: Ronsse - 2022 [7]
  - 8 neurons CPG for increased gaits diversity in quadruped robots: Liu et al. - 2025 [8]

- Follow-up work:
  - Steering implemented in Van der Noot et al. - 2019 [9]
  - Modulation of step height and length in Greiner et al. - 2018 [10]

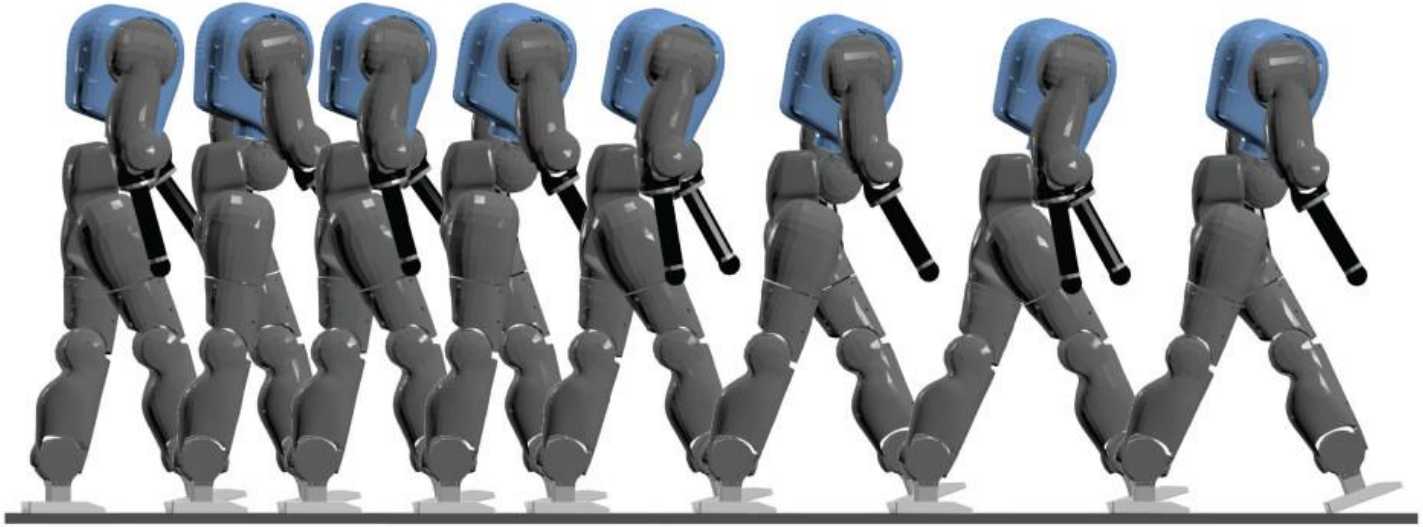

Any questions ?

“By embracing the concept of limit cycle walking, it relaxes constraints inherent to more traditional locomotion controllers.”
N. Van der Noot

References

[1] Geyer H and Herr H (2010) A muscle-reflex model that encodes principles of legged mechanics produces human walking dynamics and muscle activities. *IEEE Transactions on Neural Systems and Rehabilitation Engineering* 18(3): 263–273
[2] Matsuoka K (1985) Sustained oscillations generated by mutually inhibiting neurons with adaptation. *Biological Cybernetics* 52(6): 367–376
[3] Matsuoka K (1987) Mechanisms of frequency and pattern control in the neural rhythm generators. *Biological Cybernetics* 56(5–6): 345–353
[4] Taga G (1994) Emergence of bipedal locomotion through entrainment among the neuro-musculo-skeletal system and the environment. *Physica D: Nonlinear Phenomena* 75(1–3): 190–208
[5] Hill AV (1938) The Heat of Shortening and the Dynamic Constants of Muscle. *The Proceedings of the Royal Society of London B: Biological Sciences* 126(843): 136–195
[6] Bunz, E.K., Haeufle, D.F.B., Remy, C.D. et al. Bioinspired preactivation reflex increases robustness of walking on rough terrain. *Sci Rep* 13, 13219 (2023)
[7] Ronsse, R. (2022). Adaptive Oscillators as Template for Modeling and Assisting Rhythmic Movements. In: Torricelli, D., Akay, M., Pons, J.L. (eds) Converging Clinical and Engineering Research on Neurorehabilitation IV. ICNR 2020. Biosystems & Biorobotics, vol 28. Springer, Cham
[8] Liu Y, Liu X, Wang D, Yang W, Qu S. An eight-neuron network for quadruped locomotion with hip-knee joint control. *The International Journal of Robotics Research*. 2025;0(0)
[9] Van der Noot, N., Ijspeert, A.J. & Ronsse, R. Neuromuscular model achieving speed control and steering with a 3D bipedal walker. *Auton Robot* 43, 1537–1554 (2019)
[10] P. Greiner, N. Van Der Noot, A. J. Ljspeert and R. Ronsse, "Continuous Modulation of Step Height and Length in Bipedal Walking, Combining Reflexes and a Central Pattern Generator," *2018 7th IEEE International Conference on Biomedical Robotics and Biomechatronics (Biorob)*, Enschede, Netherlands, 2018, pp. 342-349
[11] S. Park, H. Lee and D. Lee, "Robust Motion Control of Robotic Systems with Environmental Interaction via Data-Driven Inversion of CPG," *2020 20th International Conference on Control, Automation and Systems (ICCAS)*, Busan, Korea (South), 2020, pp. 692-698